

# Freely precessing neutron stars: Model and observations

D. I. Jones<sup>1,2</sup> and N. Andersson<sup>1</sup>

<sup>1</sup> *Faculty of Mathematical Studies, University of Southampton, Highfield, Southampton, United Kingdom*

<sup>2</sup> *Department of Physics and Astronomy, University of Wales, College of Cardiff, P.O.Box 913, Cardiff, United Kingdom*

1 February 2008

## ABSTRACT

We present a model of a freely precessing neutron star which is then compared against pulsar observations. The aim is to draw conclusions regarding the structure of the star, and test theoretical ideas of crust-core coupling and superfluidity. We argue that, on theoretical grounds, it is likely that the core neutron superfluid does not participate in the free precession of the crust. We apply our model to the handful of proposed observations of free precession that have appeared in the literature. Assuming crust-only precession, we find that all but one of the observations are consistent with there not being any pinned crustal superfluid at all; the maximum amount of pinned superfluid consistent with the observations is about  $10^{-10}$  of the total stellar moment of inertia. However, the observations do not rule out the possibility that the crust and neutron superfluid core precess as a single unit. In this case the maximum amount of pinned superfluid consistent with the observations is about  $10^{-8}$  of the total stellar moment of inertia. Both of these values are many orders of magnitude less than the  $10^{-2}$  value predicted by many theories of pulsar glitches. We conclude that superfluid pinning, at least as it affects free precession, needs to be reconsidered.

**Key words:** Stars: neutron - Stars: pulsars - Stars: rotation

## 1 INTRODUCTION

This purpose of this study is to collect the important factors that influence neutron star free precession, combine them into a single unified model, and then test this model against observations. In particular, we wish to learn about the geological history of the star, decide whether or not superfluid pinning in the inner crust is required to fit the data, and ask whether it is the just the crust that participates in the free precession, or whether some (or all) of the interior neutron superfluid participates too. By ‘observations’ we refer to the handful of pulsars where a smooth modulation in the pulse timing and/or structure has been detected. We hope that the model and equations presented here will be of use to observers when new free precession candidates are discovered.

Clearly, we can only hope to extract useful information from the observations if our model of neutron star free precession is sufficiently realistic. To this end, our model includes the effects of crustal elasticity, inertial coupling (where the interior fluid pushes on the surrounding crust), and a superfluid component pinned to the inner crust. We also examine dissipative processes that tend to enforce corotation between the crust and core. We will argue that current ideas concerning crust-core coupling suggest that only the crust (and perhaps the charged plasma in the fluid core)

undergoes free precession, with the interior neutron fluid simply rotating about an axis fixed in space. This has been assumed implicitly in earlier works (Alpar & Sauls 1988), but not commented on explicitly.

The structure of this paper is as follows. In section 2 we describe how strains in a neutron star crust can provide a non-spherical contribution to the moment of inertia tensor. In section 3 we describe our free precession model. Dissipative processes which convert the precessional energy into heat or radiation are considered in section 4. In section 5 we describe how the finite crustal breaking strain places limits on the shape and wobble angle of a freely precessing star. The way in which the signal from a pulsar is modulated by free precession is described in section 6. In section 7 we combine the results of the previous sections to extract as much information as possible from the proposed observations of free precession that have appeared in the literature. Our conclusions are presented in section 8.

## 2 DEFORMATIONS OF NEUTRON STARS

To undergo free precession, a star must be deformed in some way, so that its shape and moment of inertia tensor differ from that of an unstressed fluid body. In this section we

arXiv:astro-ph/0011063v1 2 Nov 2000

describe how strain in the solid crust can provide such a deformation, using the model of Pines & Shaham (1972), who in turn made use of the terrestrial analysis as presented in Munk & McDonald (1960). For reasons of tractability a rotating but non-precessing star is considered. We will not consider deformations due to magnetic stresses, although these could be important for the free precession of very slowly rotating/very highly magnetised stars (see e.g. Melatos 1999). Note, however, that a pulsar whose deformation was due entirely to magnetic stresses would not display any modulation in its pulsations—see section 6.1.1.

Begin by writing down the total energy of the rotating star. Let  $I_{\text{star}}$  denote the moment of inertia of the spherical star, i.e. the moment of inertia the star would have if it was unstrained and not rotating. When rotating, the moment of inertia about the rotation axis must be greater than this, and so can be written as  $I_{\text{star}}(1 + \epsilon)$ . We will refer to  $\epsilon$  as the *total oblateness*. We imagine the crust to have solidified from a hot, liquid, state in the geologically distant past, leaving it with a ‘reference’ or zero-strain oblateness  $\epsilon_0$ . This parameter will then change only via crust-cracking or a gradual plastic creep. The star’s energy is a function of  $\epsilon$  and  $\epsilon_0$  according to:

$$E = E_{\text{star}} + \frac{J^2}{2I_{\text{star}}(1 + \epsilon)} + A\epsilon^2 + B(\epsilon - \epsilon_0)^2. \quad (1)$$

Here  $E_{\text{star}}$  denotes the energy the star would have if it was spherical. The second term is the kinetic energy. The third term is the increase in gravitational potential energy due to the star’s shape no longer being spherical. The fourth is the elastic strain energy, which depends quadratically on the difference between  $\epsilon$ , the actual shape of the star, and  $\epsilon_0$ . The constant  $A$  depends on the stellar equation of state, and will be of the order of the gravitational binding energy of the star. The constant  $B$  also depends on the equation of state, and will be of order of the total electrostatic binding energy of the ionic crystal lattice. The equilibrium configuration can be found by minimising the energy at fixed angular momentum:

$$\left. \frac{\partial E}{\partial \epsilon} \right|_J = 0. \quad (2)$$

For an entirely fluid star we would put  $B = 0$ , giving an oblateness of order of the ratio of kinetic and gravitational energies per unit mass:

$$\epsilon_{\text{fluid}} \approx \frac{I_{\text{star}}\Omega^2}{4A}. \quad (3)$$

Given that  $A$  is of the order of the gravitational binding energy we can write this as:

$$\epsilon_{\text{fluid}} \approx \frac{\Omega^2 R^3}{GM} \approx 2.1 \times 10^{-3} \left( \frac{f}{100 \text{ Hz}} \right)^2 R_6^3 / M_{1.4} \quad (4)$$

where  $\Omega = 2\pi f$  is the angular frequency,  $R_6$  the neutron star radius in units of  $10^6 \text{ cm}$ , and  $M_{1.4}$  the mass in units of  $1.4M_{\odot}$ .

When the strain term is included we find

$$\epsilon = \frac{I_{\text{star}}\Omega^2}{4(A + B)} + \frac{B}{A + B}\epsilon_0 \equiv \epsilon_{\Omega} + b\epsilon_0. \quad (5)$$

The oblateness is made up of two parts. The first,  $\epsilon_{\Omega}$ , scales as  $\Omega^2$  and is due to centrifugal forces. We will refer to this as the *centrifugal deformation*. The second term,  $b\epsilon_0$ , is due

entirely to the stresses of the crystalline solid, and will be referred to as the *Coulomb deformation*. We have defined  $b = B/(A + B)$ , which we will refer to as the *rigidity parameter*. It is equal to zero for a fluid star ( $B = 0$ ) and unity for a perfectly rigid one ( $B/A \rightarrow \infty$ ). Realistic neutron star equations of state imply that  $b$  takes a value of:

$$b \approx 1.6 \times 10^{-5} R_6^5 / M_{1.4}^3. \quad (6)$$

(See Jones (2000) for a simple derivation, and Ushomirsky, Cutler & Bildsten (2000) for a detailed numerical treatment). Because this is small,  $b$  is approximately equal to  $B/A$ , and so is simply the ratio of the crustal electrostatic binding energy to the total stellar gravitational binding energy. It is this second deformation that makes free precession possible, not the (possibly much larger) centrifugal deformation. We will write the total change in the moment of inertia tensor due to this Coulomb term as  $\Delta I_d$ , so that

$$\frac{\Delta I_d}{I_{\text{star}}} = b\epsilon_0. \quad (7)$$

Thus we see that the effect of elastic stresses in the crust is to change the shape only slightly from that of the corresponding fluid body. Physically, the smallness of this distortion is due to the Coulomb forces being much smaller than the gravitational and centrifugal ones.

As  $b$  is small we have  $\epsilon \approx \epsilon_{\Omega} \approx \epsilon_{\text{fluid}}$ , so that in the following sections we will use equation (4) to estimate a star’s actual oblateness. Also,  $\epsilon$  and  $\epsilon_0$  can differ at most by the breaking strain  $u_{\text{break}}$  of the crust, so we expect:

$$|\epsilon - \epsilon_0| \leq u_{\text{break}}. \quad (8)$$

This breaking strain is very poorly constrained. Estimates have ranged from  $\sim 10^{-2}$  to values very much lower—see section 5.

In the following section it will be useful to have an expression for the ratio of the crustal to total stellar moments of inertia. From Ravenhall & Pethick (1994) we find:

$$\frac{I_{\text{crust}}}{I_{\text{star}}} \approx 1.5 \times 10^{-2} R_6^4 / M_{1.4}^2. \quad (9)$$

We will approximate the total stellar moment of inertia using the constant density result

$$I_{\text{star}} = \frac{2}{5} MR^2 = 1.12 \times 10^{45} \text{ g cm}^2 M_{1.4} R_6^2. \quad (10)$$

### 3 MODELLING FREE PRECESSION

Real neutron stars will consist of an inelastic crust containing, in a non-spherical cavity, a compressible liquid core. This core will be made up of a viscous electron-proton plasma, a neutron superfluid, and possibly more exotic phases of matter also (Glendenning 1997). The crust itself may contain a pinned superfluid in its inner parts. Also, a magnetic field will thread the star, in a way which depends on the properties of the superfluid phase. The superfluid core will couple in a frictional way to the crust. The free precession of such a system will clearly be far more complicated than that of a rigid body. The strategy that has been employed to explore this free precession is to look at only one complicating factor at a time. Following this approach, we will briefly describe each complicating feature. In this section the effects of elasticity, crust-core coupling

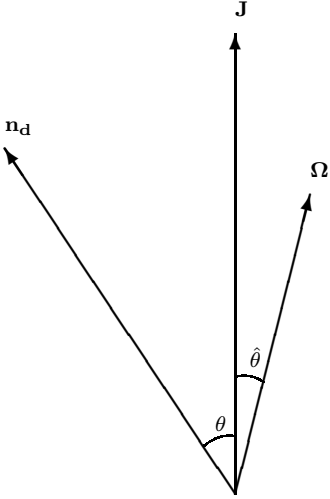


**Figure 1.** This figure shows the reference plane for a freely precessing body, which contains the deformation axis  $\mathbf{n}_d$ , the angular velocity vector  $\boldsymbol{\Omega}$  and the fixed angular momentum  $\mathbf{J}$ . The vectors  $\mathbf{n}_d$  and  $\boldsymbol{\Omega}$  rotate around  $\mathbf{J}$  at the *inertial precession frequency*  $\dot{\phi}$ . We refer to  $\theta$  as the *wobble angle*.

and superfluid pinning are described, and then combined to give a realistic free precession model. All of these complications preserve the kinetic energy of a precessing body. The dissipative effects of a frictional crust-core coupling and gravitational radiation reaction are described in section 4.

### 3.1 Rigid shell

We will begin by describing the simple case of a rigid shell. The moment of inertia tensor of any axisymmetric rigid body can be written as

$$\mathbf{I} = I_0 \boldsymbol{\delta} + \Delta I_d (\mathbf{n}_d \mathbf{n}_d - \boldsymbol{\delta}/3), \quad (11)$$

where the unit vector  $\mathbf{n}_d$  points along the body's symmetry axis. Then the principal moments are  $I_1 = I_2 = I_0 - \Delta I_d/3$ ,  $I_3 = I_0 + 2\Delta I_d/3$ , so that  $I_3 - I_1 = \Delta I_d$ . The angular momentum is then related to the angular velocity according to

$$\mathbf{J} = (I_0 - \Delta I_d/3)\boldsymbol{\Omega} - \Delta I_d \Omega_3 \mathbf{n}_d, \quad (12)$$

where the 3-axis lies along  $\mathbf{n}_d$ . This shows that the three vectors  $\mathbf{J}$ ,  $\boldsymbol{\Omega}$  and  $\mathbf{n}_d$  are always coplanar. Following Pines & Shaham (1972) we will call the plane so defined the *reference plane* (see figure 1). Given that the angular momentum is fixed, this plane must revolve around  $\mathbf{J}$ . The free precession is conveniently parameterised by the angle  $\theta$  between  $\mathbf{n}_d$  and  $\mathbf{J}$ . We will refer to this as the *wobble angle*. For a nearly spherical body the angle  $\hat{\theta}$  between  $\boldsymbol{\Omega}$  and  $\mathbf{J}$  is much smaller than the angle between  $\mathbf{J}$  and  $\mathbf{n}_d$ , according to

$$\hat{\theta} \approx \frac{\Delta I_d}{I_1} \sin \theta \cos \theta. \quad (13)$$

We will denote by  $\mathbf{n}_J$  the unit vector along  $\mathbf{J}$ . Decomposing the angular velocity according to

$$\boldsymbol{\Omega} = \dot{\phi} \mathbf{n}_J + \dot{\psi} \mathbf{n}_d \quad (14)$$

then gives

$$J = I_1 \dot{\phi}, \quad (15)$$

$$\dot{\psi} = -\frac{\Delta I_d}{I_3} \dot{\phi}. \quad (16)$$

The symmetry axis  $\mathbf{n}_d$  performs a rotation about  $\mathbf{J}$  in a cone of half-angle  $\theta$  at the angular frequency  $\dot{\phi}$ . We will refer to this as the *inertial precession frequency*. There is a superimposed rotation about the symmetry axis  $\mathbf{n}_d$  at the angular velocity  $\dot{\psi}$ . This is usually referred to as the *body frame precessional frequency*, with the corresponding periodicity known as the *free precession period*:

$$P_{\text{fp}} = \frac{2\pi}{\dot{\psi}} \quad (17)$$

For a nearly spherical body equation (16) shows that  $\dot{\psi} \ll \dot{\phi}$ , or equivalently  $P \ll P_{\text{fp}}$ . Note that the angles  $(\theta, \phi, \psi)$  are simply the usual Euler angles which describe the orientation of the rigid body (see e.g. Landau & Lifshitz 1976, figure 47).

In subsequent sections we will find it necessary to make the approximations of small wobble angle and nearly spherical stars. In this case equations (13) and (16) become:

$$\hat{\theta} \approx \frac{\Delta I_d}{I_0} \theta, \quad (18)$$

$$\dot{\psi} \approx -\frac{\Delta I_d}{I_0} \dot{\phi}. \quad (19)$$

### 3.2 Elastic shell

Following section 2, we will write the moment of inertia tensor of a rotating elastic shell as the sum of a spherical and two quadrupolar parts:

$$\mathbf{I} = I_0 \boldsymbol{\delta} + \Delta I_d (\mathbf{n}_d \mathbf{n}_d - \boldsymbol{\delta}/3) + \Delta I_\Omega (\mathbf{n}_\Omega \mathbf{n}_\Omega - \boldsymbol{\delta}/3). \quad (20)$$

(See Pines & Shaham (1972) and Munk & McDonald (1960) for further discussion). The first term on the right hand side is the moment of inertia of the non-rotating undeformed spherical shell. The second term is the change due to crustal Coulomb forces, and has the unit vector  $\mathbf{n}_d$ , fixed in the crust, as its symmetry axis. The third term is the change due to centrifugal forces, and has  $\mathbf{n}_\Omega$ , the unit vector along  $\boldsymbol{\Omega}$ , as its symmetry axis. When  $\boldsymbol{\Omega}$  moves with respect to the body the shell changes shape. This is why the shell is described as elastic.

When the directions  $\mathbf{n}_d$  and  $\mathbf{n}_\Omega$  coincide the body spins about its symmetry axis without precessing. When the two directions differ the body will precess with triaxial shape. Proceeding exactly as in the rigid body case, it is easy to prove that the elastic body undergoes a free precessional motion like that of a rigid *axisymmetric* body, with what we will call an *effective moment of inertia tensor* given by:

$$I_1 = I_0 - \Delta I_d/3 + 2\Delta I_\Omega/3, \quad (21)$$

$$I_2 = I_1, \quad (22)$$

$$I_3 = I_0 + 2\Delta I_d/3 + 2\Delta I_\Omega/3. \quad (23)$$

Crucially, the centrifugal piece of the quadrupole moment enters in a spherical way—it is only the  $\Delta I_d$  piece that is responsible for the free precession. In particular, equations (13) and (16) still apply, with  $I_1$  and  $I_3$  as given above, and

with the precession frequency and angle  $\hat{\theta}$  both proportional to the Coulomb deformation  $\Delta I_d$ .

### 3.3 Rigid shell containing non-spherical fluid

First consider the free precession of a rigid axisymmetric shell containing a *spherical* fluid cavity. We will assume that there are no viscous or frictional interactions between the shell and the fluid. In this case the free precession of the shell is exactly the same as if the fluid were not there. However, if the cavity is non-spherical, there will be a reaction force between the rigid shell and the fluid, due to the fluid tending toward a configuration symmetric about its rotational axis, and therefore ‘pushing’ on the shell. This pushing is known as *inertial coupling*. In the case of a homogeneous incompressible fluid, the combined motion of fluid and shell is given in Lamb’s monograph (1952). A number of simplifying assumptions are necessary: The motion of the fluid is always one of uniform vorticity; the ellipticity of the shell and cavity are small; and the wobble angle  $\theta$  is small.

It is then found that the shell undergoes the usual free precession motion, so that equations (18) and (19) apply, with  $\Delta I_d$  equal to the difference between the 1 and 3 principal moments of inertia of the *whole star*, not just the shell, while  $I_0$  refers to the shell only. The system’s total angular momentum  $\mathbf{J}$  is simply the sum of the angular momenta of the shell and fluid, both of which remain very nearly parallel to  $\mathbf{J}$ . As defined previously,  $\hat{\theta}$  is the angle that the angular velocity of the shell makes with  $\mathbf{J}$ . Crucially, the angular velocity of the fluid remains very close to the fixed total angular momentum of the system, i.e. *inertial coupling does not cause the fluid to participate in the free precessional motion of the shell*.

### 3.4 Rigid shell with pinned superfluid

According to many neutron star models which attempt to explain post-glitch behaviour, the neutron vortices which coexist with the inner crust become pinned, at many points along their length, to nuclei in the crustal lattice. The velocity field of this pinned superfluid is specified entirely by the distribution of these pinning sites. The pinning sites themselves are rigidly fixed to the crust. It follows that if a rigid crust is set into free precession, the instantaneous velocity field of the pinned superfluid continually adjusts, according to the orientation of the crust. Such a precessing star was studied by Shaham (1977). If we write down the angular momentum of the crust, including that of its pinned superfluid, we have

$$\mathbf{J} = \mathbf{I}\boldsymbol{\Omega} + \mathbf{J}_{\text{SF}}. \quad (24)$$

The quantities  $\mathbf{I}$  and  $\boldsymbol{\Omega}$  refer to the crust only, while  $\mathbf{J}_{\text{SF}}$  is the angular momentum of the pinned superfluid. The orientation of  $\mathbf{J}_{\text{SF}}$  is fixed with respect to the crust. We will consider only the simplest case, where all the pinned superfluid points along the crust’s deformation axis, so that  $\mathbf{J}_{\text{SF}} = J_{\text{SF}}\mathbf{n}_d$ . Then repeating the analysis of section 3.1 we find (for nearly spherical bodies with  $\theta \ll 1$ )

$$\dot{\psi} = -\frac{\Delta I}{I_0}\dot{\phi} - \frac{J_{\text{SF}}}{I_0}, \quad (25)$$

and

$$\hat{\theta} \approx \left[ \frac{\Delta I}{I_0} + \frac{J_{\text{SF}}}{J_3} \right] \theta. \quad (26)$$

In words, the pinned superfluid acts so as to increase the effective non-sphericity of an oblate body, increasing the magnitude of both the body frame precession frequency, and the misalignment between the crust’s angular momentum and angular velocity vectors.

The rotation rate of the pinned superfluid will probably be very close to the star’s rotation rate, as even a small difference between the two would give rise to a Magnus force which would break the pinning (Lyne & Graham-Smith 1998). We can therefore put  $J_{\text{SF}} \approx I_{\text{SF}}\dot{\phi}$ , where  $I_{\text{SF}}$  is the moment of inertia of the pinned superfluid. Then the above equations can be written very simply as:

$$\dot{\psi} = -\left[ \frac{\Delta I_d}{I_0} + \frac{I_{\text{SF}}}{I_0} \right] \dot{\phi} \quad (27)$$

$$\hat{\theta} \approx \left[ \frac{\Delta I_d}{I_0} + \frac{I_{\text{SF}}}{I_0} \right] \theta. \quad (28)$$

We will call the term in square brackets the *effective oblateness parameter*. It is made up of both crustal distortion and pinned superfluid parts.

### 3.5 Composite model

We now wish to consider the free precession of a more realistic composite model—an elastic shell containing a fluid cavity, with superfluid pinned to the shell. We would then form the equation of motion of the body by combining equations (20) and (24). When inertial coupling forces are neglected it is straightforward to repeat the analysis to show that the effects of elastic deformation and superfluidity add in a simple way. (Equations (27)–(28) apply, with  $\Delta I_d$  the Coulomb deformation of the shell and  $I_0$  the crustal moment of inertia). The effect of also including inertial coupling forces will be to set the  $\Delta I_d$  factor to the deformation in the moment of inertia of the *whole star*, not just the change in the crustal moment of inertia. Then equations of the form (27)–(28) apply again. In full:

$$\dot{\psi} = -\epsilon_{\text{eff}}\dot{\phi}, \quad (29)$$

$$\hat{\theta} = \epsilon_{\text{eff}}\theta, \quad (30)$$

$$\epsilon_{\text{eff}} = \frac{\Delta I_d}{I_0} + \frac{I_{\text{SF}}}{I_0}, \quad (31)$$

where  $I_0$  is equal to the crustal moment of inertia only, while  $\Delta I_d$  is the Coulomb-induced deformation in the moment of inertia of the whole star, and  $I_{\text{SF}}$  is the moment of inertia of the pinned superfluid.

## 4 DISSIPATION MECHANISMS

The model described above would, once excited, precess forever, as no dissipative energy losses have been included. A real star will suffer a number of such losses. To complete our model we will therefore consider two types of dissipation: A frictional crust-core coupling, and gravitational radiation reaction.

Before considering these particular cases we will derive a general expression for the damping timescale. The energy of the precessing crust can always be written as a function of its

angular momentum and wobble angle. For wobble damping the angular momentum of the crust is nearly constant, so we can write:

$$\dot{\theta} = \dot{E} \left/ \frac{\partial E}{\partial \theta} \right|_J. \quad (32)$$

Here  $E$  denotes the total energy of the shell plus pinned superfluid, and will include kinetic, elastic and gravitational parts. Cutler & Jones (2000) have shown that, to leading order, only the kinetic energy need be considered. It is then straightforward to take the free precession model of section 3.5 and evaluate the partial derivative of the denominator, giving

$$\dot{\theta} = \frac{\dot{E}}{\dot{\phi}^2 \theta I_0 \epsilon_{\text{eff}}}. \quad (33)$$

Expressed as a damping time this is

$$\tau_{\theta} = -\frac{\theta}{\dot{\theta}} = -\frac{\dot{\phi}^2 \theta^2 I_0 \epsilon_{\text{eff}}}{\dot{E}}. \quad (34)$$

The quantity  $\dot{E}$  will always be negative, corresponding to the conversion of mechanical energy into heat or radiation. It therefore follows that dissipation tends to decrease the wobble angle of stars with oblate deformations, but tends to increase the wobble angle of stars with prolate deformations (Cutler & Jones 2000). The crustal strains considered in this paper will almost certainly lead only to oblate deformations. More exotic scenarios (perhaps a very strong toroidal magnetic field) might lead to prolate ones. Dissipation in such stars would eventually lead to the deformation axis being orthogonal to the spin axis. Such a non-precessing triaxial star would then spin down gravitationally.

#### 4.1 Frictional crust-core coupling

We have already considered one crust-core interaction, namely inertial coupling, due to the core fluid simply ‘pushing’ on the precessing shell. However, in a real star there will be additional crust-core interactions, which have been investigated by theorists attempting to explain the post-glitch behaviour of pulsars. The core itself consists of two coexisting fluids: a plasma of electrons and protons, and a neutron superfluid. The plasma makes up only a few percent of the total mass.

The crust-core interaction proceeds in two stages. In the first stage the crust couples to the core plasma. This coupling is mediated by two separate interactions: plasma viscosity, and an electromagnetic coupling, where Alfvén waves communicate the crust’s motion to the interior. In the second stage, the plasma couples to the neutron superfluid, due to the scattering of electrons off the superfluid vortices. (Strictly, the electrons are scattered by the magnetic field created by protons which are entrained around the vortex cores; see Alpar & Sauls 1988). This second interaction is frictional in nature, i.e. is a drag force proportional to the velocity difference between the electrons and the vortices. It is sometimes referred to as ‘mutual friction’.

There will be energy losses associated with both couplings. However, following the work of Easson (1979) it is usually assumed that the crust-plasma coupling timescale is much *less* than the frictional one, so that the crust and

core plasma can be treated as a single system, interacting frictionally with the neutron core. We will work in this limit. (Relaxation of this assumption will in fact tend to strengthen our conclusion, namely that the neutron superfluid does not follow the precession of the crust).

This frictional interaction is important in two regards. Firstly, it will lead to a dissipation of the precessional energy. Secondly, if strong enough, it would cause the *whole* star—crust *and* core—to precess as a single body. We can therefore imagine two extreme cases. When the frictional coupling is very weak the crust precesses on top of a non-precessing core, with only the inertial forces of section 3.3 coupling the two. Then equation (31) applies, with  $I_0 = I_{\text{crust}}$ . At the other extreme, when the frictional forces are very strong, the star precesses as a single unit. Then equation (31) again applies, but with  $I_0 = I_{\text{star}}$ . It is clearly important to know where on this scale real neutron stars can be expected to be found, both from the point of view of modelling the precession, and for estimating the rate at which it is damped.

The motion of a rigid shell containing a spherical cavity, with a frictional coupling acting between the two, was investigated by Bondi & Gold (1955). They made the simplifying assumption that the motion of the fluid was one of rigid rotation. The shell is acted upon by a torque

$$\mathbf{T} = K(\boldsymbol{\Omega}_{\text{fluid}} - \boldsymbol{\Omega}_{\text{solid}}), \quad (35)$$

where  $K$  is a positive constant. An equal and opposite torque acts on the fluid. The equations of motion are then

$$\frac{d\mathbf{J}_{\text{shell}}}{dt} = K(\boldsymbol{\Omega}_{\text{fluid}} - \boldsymbol{\Omega}_{\text{solid}}) = -\frac{d\mathbf{J}_{\text{fluid}}}{dt} \quad (36)$$

Bondi & Gold found the normal modes of this two component system for small wobble angles. The results below can be readily found from their solution.

First consider the simple case of the non-precessing shell and fluid, rotating about the same axis, but at different rates. Using the component of the above equation along the shell’s symmetry axis, it is easy to show that the relative rotation rate decreases exponentially. We will write the e-folding time of this decay as  $n$  rotation periods, corresponding to a time  $2\pi n/\Omega$ .

Using the components of (36) orthogonal to the symmetry axis it can then be shown that in the case  $n \ll 1$  the fluid is tightly coupled to the shell, and such a body would rotate and precess as if it were a single uniform solid. In the case  $n \gg 1$  the fluid is only loosely coupled, so that while the shell undergoes free precession, the fluid’s angular velocity vector remains very nearly fixed in space.

Alpar, Langar & Sauls (1984) calculated the coupling strength for the electron-vortex core interaction described above. Using this result, Alpar & Sauls (1988) estimated  $n$  to lie in the interval  $400 \rightarrow 10^4$ . As  $n \gg 1$  it follows at once that real neutron stars lie in the weak coupling regime. In this regime it can then be shown (using the components of (36) orthogonal to the symmetry axis) that if the shell is set into free precession, with its angular momentum vector remaining along the spin axis of the fluid, the free precession is damped, with an e-folding time of  $n$  body frame free precession periods, i.e. in a time  $2\pi n/\dot{\psi}$ .

In summary, *this frictional interaction is too weak to cause the core neutron superfluid to participate in the free precession of the star’s crust. Instead, it serves only to damp*

the free precession of the crust, on a timescale of between 400 and  $10^4$  free precession periods.

#### 4.2 Gravitational radiation reaction

The effect of gravitational radiation reaction on precessing elastic bodies with a fluid non-spherical core was recently considered by Cutler & Jones (2000). It was found that the wobble angle  $\theta$  was damped exponentially on a timescale

$$\tau_g = \frac{5c^5}{2G} \frac{I_0}{(\Delta I_d)^2} \frac{1}{\Omega^4}. \quad (37)$$

This remains valid when the effects of superfluid pinning are included. Parameterising:

$$\tau_g = 1.8 \times 10^6 \text{ yr} \left( \frac{10^{43} \text{ g cm}^2}{I_0} \right) \left( \frac{10^{-6}}{\Delta I_d/I_0} \right)^2 \left( \frac{P}{1 \text{ ms}} \right)^4. \quad (38)$$

For instance, for a star with  $\Delta I_d/I_0 = \epsilon_{\text{eff}} = 10^{-6}$ ,  $I_0 = 10^{43} \text{ g cm}^2$  and  $P = 1 \text{ ms}$ , this corresponds to damping in  $n = 6 \times 10^9$  free precession periods. Comparing this with the damping rate due to friction, we see that gravitational radiation reaction is not an important source of wobble damping in any neutron star of physical interest. (This does not mean that the *spin-down* component of the radiation reaction is unimportant—see section 7.2).

### 5 CRUST FRACTURE AND MAXIMUM WOBBLE ANGLE

A real neutron star crust will have a finite breaking strain  $u_{\text{break}}$ . The actual value of this breaking strain is highly uncertain. As discussed by Ruderman (1992), extrapolations from laboratory crystals suggest that values as high as  $10^{-2}$  are possible, but the actual value may be much lower. Ruderman suggests a value of  $10^{-4}$  as plausible. For an axisymmetric star this breaking strain will limit the difference between its actual shape, which is approximately  $\epsilon_{\text{fluid}}$ , and the reference shape of the crust,  $\epsilon_0$ . However, when a star is set into free precession, additional time-dependent strains will result, even if the star is initially ‘relaxed’ (i.e.  $\epsilon_{\text{fluid}} = \epsilon_0$ ). In general, a precessing star’s crust will suffer both sorts of strain (Pines & Shaham 1972).

First consider a non-precessing spinning-down star. Its crust presumably solidified (and  $\epsilon_0$  was fixed) when it was spinning more rapidly than at present. This means its reference oblateness  $\epsilon_0$  is greater than its current actual oblateness  $\epsilon_{\text{fluid}}$ , so that we would now expect  $\epsilon_0 > \epsilon_{\text{fluid}}$ . Combining with the bound due to crust fracture we then have

$$0 < \epsilon_0 - \epsilon_{\text{fluid}} < u_{\text{break}}. \quad (39)$$

Even if the crust has cracked a number of times during spin-down we would still expect the star to have some ‘memory’ of its initial shape (unless the cracking was able to relieve *all* the stresses in the crust), so that the above equation should still hold.

In the case of an accreting star the situation is different. If the star has been spun up from a relaxed state at a small rotation rate we would expect its current oblateness  $\epsilon_{\text{fluid}}$  to *exceed* its reference oblateness  $\epsilon_0$ . However, the accretion will tend to create new crustal material relaxed to the current

rotation rate of the star, so that the difference  $\epsilon_{\text{fluid}} - \epsilon_0$  may be rather small.

We will now look at the opposite case, when the strains are *due to precession only*, i.e. when  $\epsilon_0 = \epsilon_{\text{fluid}}$ . A simple treatment is possible, based upon the known geometry of free precession for an elastic body, as discussed in section 3.2. These strains can be used to place a limit on the maximum possible wobble angle  $\theta$  a star can sustain.

We know that (for small wobble angles at least) when an initially axially symmetric body is set into free precession a deformation  $\Delta I_d$  remains along the axis  $\mathbf{n}_d$  fixed in the star, while a deformation  $\Delta I_\Omega$  points along the angular velocity vector. From the point of view of an observer attached to the crust, a deformation of size  $\Delta I_\Omega$  describes a cone of half-angle  $\theta + \hat{\theta} \approx \theta$  about  $\mathbf{n}_d$ . This change in shape is all we need to know to estimate the strain: The change in position of any given particle is of order  $R\epsilon_\Omega\theta$ , while the corresponding strain is of order  $\epsilon_\Omega\theta$ . This precession-induced strain is not constant, but varies with magnitude  $\epsilon_\Omega\theta$  over one (body frame) free precession period. As there exists a maximum strain  $u_{\text{break}}$  that the solid can withstand prior to fracture, the wobble angle will be limited to a value of  $u_{\text{break}}/\epsilon_\Omega \approx u_{\text{break}}/\epsilon_{\text{fluid}}$  so that:

$$\theta_{\text{max}} \approx 0.45 \left( \frac{100 \text{ Hz}}{f} \right)^2 \left( \frac{u_{\text{break}}}{10^{-3}} \right) \text{ radians}. \quad (40)$$

Qualitatively, we can say that faster spinning neutron stars have larger bulges to re-orientate and therefore can sustain smaller wobble angles prior to fracture. For sufficiently slowly spinning stars the above equation breaks down, yielding angles in excess of  $\pi/2$ . The wobble angles of such slowly spinning stars are not limited by crustal strain. To give two extreme examples, for a breaking strain of  $10^{-3}$  the wobble angle of a 300Hz neutron star in a low-mass X-ray binary or millisecond pulsar would be limited to about  $3^\circ$ , while a ‘standard’ field pulsar spinning at around a Hz could precess with *any* wobble angle.

We therefore have two separate bounds that a freely precessing star must satisfy, one due to the mismatch between its reference and actual shape, and one due to free precession. These bounds will be of use in section 7, when we examine possible observations of free precession.

### 6 EFFECT OF FREE PRECESSION ON THE PULSAR SIGNAL

In this section we will examine the effect of free precession on the electromagnetic signal of a pulsar. The aim is to describe how free precession might be detected using electromagnetic data, by examining variations in the pulse frequency, amplitude and polarisation. From these we hope to test our free precession model and extract information concerning the wobble angle, effective oblateness and superfluid pinning.

In section 6.1 we will consider the problem of how the precession affects the electromagnetic pulses for a torque-free top. This calculation requires only the geometry of free precession, and we will refer to these modulations as the purely geometric modulations. However, real pulsars are acted on by electromagnetic spin-down torques. The magnitude of these torques will themselves be modulated by the

free precession, although the form of the modulation depends on the model of spin-down torque employed. These torques will, in turn, modify the pulsations. In section 6.2 we will include these variable torques using a simple spin-down model.

Some of the results given here have been presented previously, in varying degrees of generality. We hope that by assembling all of the important observational characteristics of free precession in one place, we will provide a resource for observers wishing to assess the likelihood of a given pulse modulation being caused by free precession.

### 6.1 Effect of free precession on the pulsar signal: Geometric effects

We will begin by modelling the neutron star as a torque-free precessing symmetric top. We will model the pulsations in the obvious way, i.e. as a thin beam fixed with respect to the star's body axes, aligned with the dipole moment  $\mathbf{m}$ . Each pulsation then corresponds to the passage of  $\mathbf{m}$  through the plane containing the angular momentum vector  $\mathbf{J}$  and the observer. The motion of  $\mathbf{m}$  is then a slow rotation at  $\dot{\psi}$  about  $\mathbf{n}_d$ , the deformation axis, superimposed on the rapid rotation of  $\mathbf{n}_d$  at  $\dot{\phi}$  about  $\mathbf{J}$ . This will lead to variations in the pulse phase, amplitude and polarisation, on the body frame precession timescale  $P_{\text{fp}} = 2\pi/\dot{\psi}$ . We will begin by considering the phase variations.

#### 6.1.1 Phase modulation

The problem of phase modulation due to precession was first considered by Ruderman (1970), and has been elaborated upon since by Bisnovatyi-Kogan et al. (1990) and Bisnovatyi-Kogan & Kahabka (1993) in connection with the 35 day periodicity observed in Her X-1. Following the discovery of planets around pulsar PSR 1257+12 a number of authors re-examined the issue to check whether or not free precession could mimic planetary perturbations of the pulsation (Nelson, Finn & Wasserman 1990; Cordes 1993; Gil et al. 1993; Glendenning 1995). We will comment upon their findings in section 6.2.

Let  $\hat{\mathbf{m}}$  denote a unit vector along  $\mathbf{m}$ . Denote the orientation of the body frame axes  $\{\hat{x}, \hat{y}, \hat{z}\}$  with respect to the inertial frame axes  $\{x, y, z\}$  by the usual Euler angles  $(\theta, \phi, \psi)$ . (See figure 47 of Landau & Lifshitz 1976). Let  $\hat{\mathbf{m}}$  lie in the  $\hat{x}\hat{z}$  plane, at an angle  $\chi < \pi/2$  to the  $\hat{z}$ -axis. Then the components  $[\hat{m}_x, \hat{m}_y, \hat{m}_z]$  of  $\hat{\mathbf{m}}$ , referred to the inertial frame are

$$\begin{bmatrix} \cos \phi \cos \psi \sin \chi - \sin \phi \cos \theta \sin \psi \sin \chi + \sin \phi \sin \theta \cos \chi \\ \sin \phi \cos \psi \sin \chi + \cos \phi \cos \theta \sin \psi \sin \chi - \cos \phi \sin \theta \cos \chi \\ \sin \theta \sin \psi \sin \chi + \cos \theta \cos \chi \end{bmatrix}$$

Define Euler-like angles  $\Theta$  and  $\Phi$  to describe the polar angle and azimuth of  $\hat{\mathbf{m}}$ . Then the  $\Phi$  angle describes the phase of the pulsar signal, with a pulsation being observed whenever  $\Phi$  is equal to the azimuth of the observer, e.g. whenever  $\Phi = 0$  for an observer in the inertial  $x > 0, z > 0$  quarter-plane. Then

$$\tan \Phi = \frac{\hat{m}_y}{\hat{m}_x}. \quad (41)$$

A little algebra leads to

$$\Phi = \phi - \frac{\pi}{2} + \arctan \left[ \frac{1}{\cos \theta} \left( \frac{\cos \psi \tan \chi}{\tan \theta - \sin \psi \tan \chi} \right) \right] \quad (42)$$

and also

$$\dot{\Phi} = \dot{\phi} + \dot{\psi} \sin \chi \frac{\cos \theta \sin \chi - \sin \psi \sin \theta \cos \chi}{(\sin \theta \cos \chi - \cos \theta \sin \psi \sin \chi)^2 + \cos^2 \psi \sin^2 \chi}, \quad (43)$$

where  $\dot{\Phi}$  is the *instantaneous electromagnetic frequency*. Its time-averaged value is what we would normally refer to as the 'spin frequency' of the star, which we will denote by  $\Omega$ . In order to proceed it is necessary to treat the  $\theta > \chi$  and  $\theta < \chi$  cases separately.

#### $\theta > \chi$ case

First consider the *average* electromagnetic pulse frequency. An increase of  $\phi$  by  $2\pi$  at fixed  $\psi$  causes  $\hat{\mathbf{m}}$  to rotate once about  $\mathbf{J}$ , i.e. causes a pulsation. However, an increase in  $\psi$  by  $2\pi$  at fixed  $\phi$  *does not* rotate  $\hat{\mathbf{m}}$  about  $\mathbf{J}$ , i.e. does not cause a pulsation. It follows that the *average* electromagnetic frequency is exactly  $\dot{\phi}$ . The departure from this average spin rate can best be expressed as a phase residual  $\Delta\Phi$ :

$$\Delta\Phi = \Phi - \left(\phi - \frac{\pi}{2}\right) \quad (44)$$

$$= \arctan \left[ \frac{1}{\cos \theta} \left( \frac{\cos \psi \tan \chi}{\tan \theta - \sin \psi \tan \chi} \right) \right]. \quad (45)$$

The denominator of the term in curved brackets is clearly non-zero for all  $\psi$ , and so  $\Delta\Phi$  remains in the range  $-\pi/2 < \Delta\Phi < \pi/2$  (Nelson, Finn & Wasserman 1990). In the case  $\theta \gg \chi$  we find

$$\Delta\Phi = \frac{\chi}{\sin \theta} \cos \psi \quad (46)$$

and

$$\Delta\dot{\Phi} = -\dot{\psi} \frac{\chi}{\sin \theta} \sin \psi \quad (47)$$

When  $\chi = 0$ , as would be the case for a star whose deformation is due entirely to axisymmetric magnetic stresses, there is no modulation in the pulsations at all. The free precession of such a star would only be detectable if there was some non-axisymmetry in the pulsar beam.

#### $\theta < \chi$ case

As described in section 5, the wobble angles of rapidly rotating stars are limited to small values by the finite crustal breaking strain, so that for such stars this is almost certainly the case of interest. Again begin by considering the average pulsation frequency. An increase of  $\phi$  by  $2\pi$  at fixed  $\psi$  causes  $\hat{\mathbf{m}}$  to rotate once about  $\mathbf{J}$ , i.e. causes a pulsation. It is also the case that an increase of  $\psi$  by  $2\pi$  at fixed  $\phi$  causes  $\hat{\mathbf{m}}$  to rotate once about  $\mathbf{J}$ , i.e. causes a pulsation. It follows that the average pulsation frequency is  $\dot{\phi} + \dot{\psi}$ . The phase residual is now given by

$$\Delta\Phi = \Phi - (\phi + \psi) \quad (48)$$

$$= \arctan \frac{(\cos \theta - 1) \sin \psi \sin \chi - \sin \theta \cos \chi}{\cos \psi \sin \chi + (\cos \theta \cos \psi \sin \chi - \sin \theta \cos \chi) \tan \psi}.$$

It is straightforward to show that the denominator of this function is non-zero for all  $\psi$ , and so  $\Delta\Phi$  remains in the range  $-\pi/2 < \Delta\Phi < \pi/2$  (Nelson, Finn & Wasserman 1990).

When  $\theta \ll \chi$  we find

$$\Delta\Phi = -\theta \frac{\cos\chi}{\sin\chi} \cos\psi \quad (49)$$

and

$$\Delta\dot{\Phi} = \dot{\psi}\theta \frac{\cos\chi}{\sin\chi} \sin\psi. \quad (50)$$

We therefore see that for small wobble angles the phase residual varies sinusoidally on the (long) free precession timescale, with an amplitude  $\theta$ . The fractional variation in pulsation frequency is of order  $\theta\dot{\psi}/\dot{\Phi} \sim \theta\epsilon_{\text{eff}}$ .

### 6.1.2 Amplitude modulation

The precessional motion will modulate the amplitude of the pulsar signal, although the precise form of the modulation will depend upon the geometry of the emission region. Assuming emission axisymmetry about the dipole axis and that the intensity of emission falls off over an angular width  $W$ , the fractional change in amplitude  $\Delta A/A$  due to precessional modulation is of order (Cordes 1993)

$$\frac{\Delta A}{A} \approx \frac{\Delta\Theta}{W}, \quad (51)$$

where  $\Delta\Theta$  denotes the change in polar angle of  $\hat{\mathbf{m}}$  over a free precession period. We have

$$\cos\Theta = \hat{\mathbf{m}}_z = \sin\theta \sin\psi \sin\chi + \cos\theta \cos\chi, \quad (52)$$

from which we find the (obvious) results that  $\Theta$  has a maximum value of  $\chi + \theta$  and a minimum value of  $|\chi - \theta|$ . It follows that  $\Delta\Theta$  is approximately equal to  $\theta$  or  $\chi$ , whichever is smaller.

Pulsar duty cycles (i.e. angular widths of the beam) are typically of order of  $10^\circ$  (Lyne & Graham-Smith 1998), so we will parameterise according to

$$\frac{\Delta A}{A} \approx 6 \times 10^{-3} \left( \frac{\theta}{10^{-3}} \right) \left( \frac{10^\circ}{W} \right), \quad (53)$$

assuming  $\theta < \chi$ . This modulation will occur at the body frame free precession frequency.

### 6.1.3 Polarisation modulation

As above, we will assume a pulsar beam structure symmetric about  $\hat{\mathbf{m}}$ . In addition, we will take the polarisation model described in Lyne & Graham-Smith (1998, section 12.2). In this model the polarisation vector of the observed radiation is parallel to the magnetic field line where the radiation was produced. Then the time variation of the linear polarisation angle,  $\lambda$ , can be calculated (see their equation 12.2). It is this quantity that is measured by observers. In the absence of free precession this angle varies rapidly at the spin frequency. Free precession will cause an additional modulation at precession period  $P_{\text{fp}}$ . A useful diagnostic for observers is the maximum rate of change of this angle with time,  $\dot{\lambda}_{\text{max}}$ , which occurs when the dipole axis lies closest to the observers line-of-sight. Let  $i$  denote the inclination angle, i.e.

the angle between  $\mathbf{J}$  and the line-of-sight. Using the equation of Lyne & Graham-Smith for  $\lambda$  we then find (for  $\theta < \chi$ ) a fractional modulation in  $\dot{\lambda}_{\text{max}}$  of

$$\frac{\Delta\dot{\lambda}_{\text{max}}}{\dot{\lambda}_{\text{max}}} = \frac{2 \sin i}{\sin\chi \sin(i-\chi)} \theta. \quad (54)$$

## 6.2 Effect of free precession on the pulsar signal: Electromagnetic torque effects

The calculations of section 6.1 considered a precessing symmetric top entirely free of torques. However, the fact that the star is visible as a pulsar means that it will be acted upon by an electromagnetic torque, and this should be included in the calculation. This torque will not affect the amplitude and polarisation arguments. However, provided that the torque is a function of the spin rate and orientation of  $\mathbf{m}$ , i.e. of  $\dot{\Phi}$  and  $\Theta$ , the spin-down torque will be modulated by the precession. This modulation in the torque must be taken into account when calculating the phase residuals. We will call this *electromagnetic* modulation. The affect on the phase residuals of this varying torque has been considered analytically by Jones (1988) and Cordes (1993) for general torque functions, and numerically by Melatos (1999) for the Deutsch (1955) torque. We, however, will give a simple description based on the vacuum point-dipole spin-down torque so that

$$\ddot{\Phi} = k\dot{\Phi}^3 \sin^2\Theta, \quad (55)$$

where  $k$  is a negative constant. The fractional change in spin-down rate due to precession is given by

$$\frac{\Delta\ddot{\Phi}}{\ddot{\Phi}} \approx 3 \frac{\Delta\dot{\Phi}}{\dot{\Phi}} + 2 \frac{\Delta(\sin\Theta)}{\sin\Theta}. \quad (56)$$

The prefix  $\Delta$  denotes the departure of the respective quantity from the smooth non-precessing power law spin-down. We will consider the case  $\theta < \chi$ . From equation (50) we see that the first term is of order  $\epsilon_{\text{eff}}\theta$ . Using equation (52) it is easy to show that

$$\sin^2\Theta \approx \sin^2\chi - 2\theta \sin\chi \cos\chi \sin\psi \quad (57)$$

so that the second term of (56) is of order  $\theta$ , and therefore is the dominant one. We then have

$$\Delta\ddot{\Phi} \approx -2k\Omega^3\theta \sin\chi \cos\chi \sin\psi. \quad (58)$$

All the quantities on the right hand side are constant, apart from the angle  $\psi$ , which is a linear function of time:  $\psi = \dot{\psi}t$ . We can integrate once to get the perturbation in frequency

$$\Delta\dot{\Phi} \approx 2k\Omega^3 \sin\chi \cos\chi \cos\psi \frac{\theta}{\dot{\psi}}, \quad (59)$$

and once more to obtain the phase residual

$$\Delta\Phi \approx 2k\Omega^3 \sin\chi \cos\chi \sin\psi \frac{\theta}{\dot{\psi}^2}. \quad (60)$$

Now use  $|\dot{\psi}/\dot{\Phi}| = \epsilon_{\text{eff}}$  to give

$$\Delta\Phi = \frac{1}{\pi} \cot\chi \frac{\theta}{\epsilon_{\text{eff}}^2} \frac{P}{\tau_e}, \quad (61)$$

where  $P$  denotes the spin period and  $\tau_e = |\ddot{\Phi}/\dot{\Phi}|$  is the spin-down timescale. For example, if we consider a star where superfluid pinning is not operative, and where only



the crust participates in the free precession, we can put  $\epsilon_{\text{eff}} \approx b\epsilon_{\Omega}I_{\text{star}}/I_{\text{crust}}$  (assuming  $\epsilon_0 \approx \epsilon_{\text{fluid}}$ ) to give

$$\Delta\Phi = 25 \cot \chi \left( \frac{\theta}{10^{-3}} \right) \left( \frac{10^{-5}}{b} \right)^2 \left( \frac{P}{30 \text{ ms}} \right)^3 \left( \frac{10^3 \text{ yrs}}{\tau_e} \right) \left( \frac{I_{\text{crust}}/I_{\text{star}}}{0.015} \right)^2. \quad (62)$$

We have parameterised with a young pulsar in mind. This should be compared with the torque-free residual of equation (49). We see that for the parameterisation above the electromagnetic torque variation has greatly amplified the residual. Note, however, that for millisecond pulsars which have  $\tau_e \lesssim 10^9$  years the torque variations are unimportant.

Note also that for the parameterisations above, as  $\Delta\Phi$  is greater than  $2\pi$ , this phase variation makes it difficult to detect such pulsars—any search algorithm that integrates radio data assuming a constant frequency source will go out of phase with the signal in an interval of the order of the free precession period. However, pulsar physicists do take such a modulation into account when performing data analysis when they search for binary pulsars, as a sinusoidal phase variation is also produced by a binary orbit: Small-angle free precession and nearly-circular binary orbits *both* produce sinusoidal phase residuals, to leading order in wobble angle and orbital eccentricity, respectively. As pointed out by Nelson et al. (1990), in order to distinguish between the two models it is necessary to include higher order terms. Then the residuals have different forms, allowing differentiation between the two models. Also, free precession will almost certainly lead to an amplitude modulation in phase with the timing residuals, whereas a binary companion would only produce amplitude modulation if it happened to cut the observer’s line-of-sight onto the pulsar beam, providing another means of differentiation.

We will present the phase residual in one more form. If we put  $\dot{\psi} = 2\pi/P_{\text{fp}}$  we obtain

$$\Delta\Phi = \frac{1}{\pi} \cot \chi \left( \frac{P_{\text{fp}}}{P} \right) \left( \frac{P_{\text{fp}}}{\tau_e} \right) \theta. \quad (63)$$

## 7 ANALYSIS OF OBSERVATIONS OF FREE PRESSION

Having set out our free precession model in some detail, and described how free precession modulates the electromagnetic signal of a pulsar, we will now turn to the problem of extracting useful information from the pulsar observations. First we will assemble the necessary equations.

### 7.1 Formulae required to extract source parameters from observations

The problem divides into two parts: Extracting the wobble angle  $\theta$ , and extracting information concerning the structure of the star, such as its reference shape or the amount of pinned superfluid.

The extraction of the wobble angle is relatively straightforward. We need only invert the equations of the previous section. Comparing the geometric phase residual of equation (49) with the electromagnetic torque residual of equation

(63), we see that the electromagnetic torque significantly amplifies the geometric residual when

$$\frac{1}{\pi} \left( \frac{P_{\text{fp}}}{P} \right) \left( \frac{P_{\text{fp}}}{\tau_e} \right) \gg 1. \quad (64)$$

When this equality is satisfied equation (63) applies, and the wobble angle can be extracted (up to a factor of  $\tan \chi$ ) from the observed values of spin period, free precession period and phase residual magnitude according to

$$\theta = \pi \left( \frac{P}{P_{\text{fp}}} \right) \left( \frac{\tau_e}{P_{\text{fp}}} \right) \Delta\Phi \tan \chi. \quad (65)$$

Note that if the spin-down torque is a steeper function of  $\Theta$  than the vacuum dipole model predicts (equation 55) the wobble angle as estimated by the above equation will be an overestimate. If the torque is not as steep as assumed, then the calculated wobble angle will be an underestimate.

When the inequality is reversed the phase residuals are described accurately by the geometric variation, and equation (49) applies. Then the wobble angle can be extracted (up to a factor of  $\tan \chi$ ) from the value of  $\Delta\Phi$  according to

$$\theta = \Delta\Phi \tan \chi. \quad (66)$$

Information concerning the structure of the star is more difficult to obtain. We hope to extract this information from equation (31), where the quantity  $\epsilon_{\text{eff}}$  is simply the ratio of spin and modulation periods,  $P/P_{\text{fp}}$ . Ideally, we would like to extract the three quantities  $\Delta I_{\text{d}}$  (the deformation in the moment of inertia tensor caused by Coulomb forces),  $I_{\text{SF}}$  (the moment of inertia of the pinned superfluid), and  $I_0$  (the part of the moment of inertia which participates in the free precession). Clearly, the problem is underdetermined. However, the quantity  $\Delta I_{\text{d}}/I_{\text{star}}$  is, for a given oblateness  $\epsilon_0$ , constrained by the equation of state according to equation (7), so that:

$$\epsilon_{\text{eff}} = \frac{P}{P_{\text{fp}}} = b\epsilon_0 \frac{I_{\text{star}}}{I_0} + \frac{I_{\text{SF}}}{I_0}. \quad (67)$$

The problem then becomes one of extracting  $\epsilon_0$ ,  $I_{\text{SF}}$ , and  $I_0$ . The quantity  $\epsilon_0$  is, for a spinning-down star, almost certainly greater than or equal to the actual oblateness  $\epsilon_{\text{fluid}}$  (given by equation 4), and cannot exceed  $\epsilon_{\text{fluid}}$  by more than  $u_{\text{break}}$ . Also, if our understanding of crust-core coupling is correct,  $I_0$  is simply the crustal moment of inertia. Given these assumptions, the above equation can be used to place limits on  $I_{\text{SF}}$ , the least certain of all the stellar parameters.

However, we will employ a slightly simpler strategy, for the following reason: If, as some glitch theories require, a few percent of the stars’ moment of inertia was made up of a superfluid pinned to the inner crust, the effective oblateness parameter would be of order unity, so that  $P_{\text{fp}} \sim P$ . If the observations below really do represent free precession, this prediction has failed completely. We will therefore proceed as follows. We will begin by setting  $I_{\text{SF}}$  to zero, allowing us to extract a reference oblateness:

$$\epsilon_0 = \epsilon_{\text{eff}} \frac{1}{b} \frac{I_0}{I_{\text{star}}} \quad (I_{\text{SF}} = 0 \text{ limit}). \quad (68)$$

In the case where  $I_0 = I_{\text{crust}}$  we can use equations (6) and (9) to give:

$$\epsilon_0 = 10^3 \epsilon_{\text{eff}} \frac{M_{1.4}}{R_6} \quad (I_{\text{SF}} = 0 \text{ limit}). \quad (69)$$

This can then be tested against inequality (39). There are three possible cases.

Case I: If the inequality is violated because  $\epsilon_0 < \epsilon_{\text{fluid}}$ , our model requires modification. The most likely modification is that more than just the crust participates in the motion, so that  $I_0 > I_{\text{crust}}$ . This would be a sign of stronger crust-core coupling than anticipated. Setting  $I_{\text{SF}}$  to a non-zero value would only serve to increase  $I_0$ .

Case II: If the inequality is satisfied, then the observation is consistent with superfluid pinning not playing a role in free precession. The possibility that superfluid pinning is making up some part of the total  $\epsilon_{\text{eff}}$  remains, but  $I_{\text{SF}}/I_0$  can be no larger than  $\sim \epsilon_{\text{eff}}$ .

Case III: The inequality is violated because  $\epsilon_0 - \epsilon_{\text{fluid}} > u_{\text{break}}$ . Of course,  $u_{\text{break}}$  is unknown, but is surely less than  $10^{-2}$  (Ruderman 1992). If the inequality is violated even for this large breaking strain, then superfluidity is playing the dominant role in determining the free precession frequency. In this case  $\epsilon_{\text{eff}} \sim I_{\text{SF}}/I_0$ , or equivalently

$$\frac{I_{\text{SF}}}{I_{\text{star}}} = \epsilon_{\text{eff}} \frac{I_0}{I_{\text{star}}} \quad (\epsilon_0 = 0 \text{ limit}). \quad (70)$$

Again parameterising with  $I_0 = I_{\text{crust}}$  using equation (9) we obtain:

$$\frac{I_{\text{SF}}}{I_{\text{star}}} = 1.5 \times 10^{-2} \epsilon_{\text{eff}} \frac{R_6^4}{M_{1.4}^2} \quad (\epsilon_0 = 0 \text{ limit}). \quad (71)$$

## 7.2 Analysis of observations

We will now apply our free precession model to the proposed observations of free precession to have appeared in the literature. The collection below does not represent *all* of the proposed candidates: We have not included observations where only the (proposed) free precession timescale  $P_{\text{fp}}$  has been measured, and not the (average) spin period  $P$ . Also, we have not included sources where only one modulation cycle in the pulsations (or less) has been observed. In restricting our sample in this way, we will confine our attention to sources where the evidence for a modulation in the pulsations is reasonably secure, and where the observational data is good enough for source parameters to be estimated.

### PSR B0531+21 (The Crab pulsar)

Lyne, Pritchard and Smith (1988) observed a variation in the phase residual of the Crab pulsar of about 1.9 radians, with period 20 months. Jones (1988) suggested free precession as the cause, and pointed out that the residuals would be dominated by the electromagnetic torque variation. Equation (65) then gives  $\theta \approx 5 \times 10^{-6} \tan \chi$  radians.

Equation (69) gives a reference oblateness of  $6 \times 10^{-7}$ , while equation (4) gives  $\epsilon_{\text{fluid}} = 2 \times 10^{-4}$ . This violates the inequality (39) (case I)—the star would seem to have a reference shape much less oblate than its current actual shape. Even if the whole star is assumed to participate in the free precession, so that  $I_0 = I_{\text{star}}$ , we find  $\epsilon_0 = 4.3 \times 10^{-5}$  (equation 68), so that inequality (39) is still violated. Therefore, it is not possible to make this observation fit our free precession model for any sensible stellar parameters. Given that the modulation has not been detected in subsequent observations, it seems unlikely that free precession was detected.

More recently, evidence has been presented for a 60s modulation in the Crab pulsar's amplitude and phase residual, both in the optical band (Čadež & Galičič 1996a; Čadež & Galičič 1996b; Čadež & Galičič & Calvani 1997). This is by far the shortest free precession period to have been proposed in the literature. Čadež & Galičič report a phase residual amplitude of  $\Delta\Phi = 1.2 \times 10^{-3}$  radians. For  $P_{\text{fp}} = 60$ s electromagnetic torque amplification is insignificant. Equation (66) gives  $\theta \approx 1.2 \times 10^{-3} \tan \chi$  radians. They also report a fractional amplitude modulation of  $6 \times 10^{-3}$ . Equation (53) then gives  $\theta \approx 1.1 \times 10^{-4}$ . These two  $\theta$  estimates would agree for  $\chi \sim 0.1$  radians.

In the absence of pinning, equation (69) gives a reference oblateness of 0.55. This is a large value, violating (39) (case III) even for  $u_{\text{break}} = 10^{-2}$ . In other words, the reference oblateness is too large to be accounted for by Coulomb deformation alone. It is therefore necessary to invoke superfluid pinning: Using equation (71), we see a fraction of order  $10^{-5}$  of the star's moment of inertia needs to be pinned to fit the data. However, a subsequent search (Golden et al. 2000) has failed to confirm the modulation, weakening the precession hypothesis.

### PSR B0833-45 (The Vela pulsar)

Deshpande & McCulloch (1996) have presented evidence for a 165d variation in the Vela's amplitude in the radio band. The fractional modulation is of order 1/2. They have also investigated the difference in time-of-arrival of the pulses at two different radio frequencies, and found a 330d variation. The most natural explanation of this latter variation, and probably therefore of the former too, would be connected with refractive scintillations (Lyne & Graham-Smith 1998) due to the inter-stellar medium. However, the authors suggested free precession as the cause. It is not easy to see how precession could cause the variation in the time-of-arrival difference between the radio frequencies. We will therefore concentrate on the amplitude variation. Equation (53) gives  $\theta \approx 0.1$  radians  $\approx 6^\circ$ .

Assuming no superfluid pinning, the 165d modulation in the Vela gives a reference oblateness of  $\epsilon_0 = 6 \times 10^{-6}$ , a factor of 4 less than the calculated actual oblateness,  $\epsilon_{\text{fluid}} = 3 \times 10^{-5}$ . We therefore see that the inequality (39) is violated (case I)—the star is more nearly spherical than we would expect. In order to increase  $\epsilon_0$  to its minimum acceptable value of  $\epsilon_{\text{fluid}}$ , at least 6% of the star would need to participate in the free precession. Inclusion of superfluid pinning increases this value.

### PSR B1642-03

Cordes (1993) has reported evidence for  $10^3$ d variations in the pulse shape and timing residuals of pulsar B1642-03, both in the radio band. Three cycles have been observed (see figure VI of his paper), although the profile is far from sinusoidal. The fractional pulse shape modulation was approximately 0.05, so that equation (53) leads to  $\theta \approx 9 \times 10^{-3}$  radians. The phase residual amplitude is difficult to identify as it seemed to increase over the observation period, but a value  $\Delta\Phi \approx 0.025$  is a reasonable average. This pulsar has residuals dominated by the electromagnetic torque variation

(equation 64), so that equation (65) gives  $\theta \approx 8 \times 10^{-4} \tan \chi$  radians. These two estimates are consistent for  $\chi \approx 0.1$  radians.

For the reference oblateness in the zero pinning limit, equation (69) gives  $\epsilon_0 = 5 \times 10^{-6}$ , while equation (4) gives  $\epsilon_{\text{fluid}} = 10^{-6}$ , so that inequality (39) is satisfied (case II). Therefore, this observation is consistent with zero superfluid pinning. The calculated reference oblateness is very close to the actual shape, suggesting that the star is virtually unstrained. This could imply a very low crustal breaking strain of order  $10^{-6}$ . The pinned superfluid component can make up no more than  $10^{-10}$  of the total stellar moment of inertia.

### PSR B1828-11

Very recently a 1009d periodicity has been reported in the radio shape and residuals of pulsar B1828-11 (Stairs et al. 2000). Approximately four cycles have been observed. The pulse width is about  $3^\circ$ , and the pulse shape changes drastically over one free precession period, suggesting  $\theta \sim 3^\circ$ .

The phase residuals give, via equation (65), a wobble angle of only  $3.5 \times 10^{-4}$  radians =  $0.02^\circ$ , two orders of magnitude less. However, as is immediately apparent, there is a very strong 504d periodicity in the data. If we put  $P_{\text{fp}} = 504\text{d}$  we obtain a  $\theta = 0.08^\circ$ , still a factor of order 30 too small to agree with the wobble angle derived from the amplitude modulation. (Stairs et al. obtain  $0.3^\circ$  using a similar method of calculation, still one order of magnitude smaller than the amplitude-derived value). There is clearly a problem in extracting the wobble angle of the source.

However, the fact that the data contains a strong periodicity at 504d strongly suggests the following: The free precession period is indeed 1009 days, but the magnetic dipole lies very nearly orthogonal to the star's deformation axis, i.e.  $\chi \approx \pi/2$ . Then both the phase modulation of equation (48) and the amplitude modulation connected with equation (52) have significant components at  $2\dot{\psi}$ . To show this expand these equations to second order in  $\theta$ . For the phase modulation:

$$\Delta\Phi = -\theta \cot \chi \cos \psi - \frac{1}{4}\theta^2 \sin 2\psi(1 + 2 \cot^2 \chi), \quad (72)$$

where the time dependence of the right hand side is due to  $\psi = \dot{\psi}t$ . The first term is the linear (in  $\theta$ ) phase modulation at  $\dot{\psi}$ , and the second the quadratic (in  $\theta$ ) phase modulation at  $2\dot{\psi}$ . The amplitude modulation for an unmagnetised star is due to the variation in  $\Theta$  given by

$$\sin^2 \Theta = \sin^2 \chi + \theta^2 \cos 2\chi - 2 \sin \chi \cos \chi \sin \psi \theta - \frac{1}{2}\theta^2 \sin^2 \chi \cos 2\psi. \quad (73)$$

The first two terms are uninteresting constants, the third the linear phase modulation at  $\dot{\psi}$ , and the last the quadratic phase modulation at  $2\dot{\psi}$ . The quadratic terms in (72) and (73) dominate the linear ones when:

$$\tan \chi > \frac{4}{\theta}. \quad (74)$$

The calculation of section 6.2 for the phase modulation for a magnetised star can then be repeated. In the  $\chi \rightarrow \pi/2$  limit we obtain

$$\Delta\Phi = \frac{1}{4\pi} \frac{P_{\text{fp}}^2}{\tau_e P} \theta^2 \cos 2\psi \quad (75)$$

We can then invert this relation to give the wobble angle. Using  $P_{\text{fp}}$  gives  $\theta = 2^\circ$ , in excellent agreement with the value estimated using the amplitude modulation. For consistency  $\chi$  must then satisfy (74), which gives  $\chi > 89^\circ$ . In other words, for this scenario to apply, we require near perfect orthogonality between the deformation axis and the magnetic dipole axis.

The spin and modulation periods of this star are, by coincidence, almost identical to those reported above for PSR B1642-03, so the same conclusions regarding the star's structure can be drawn, *viz* that the observation is consistent with our free precession model, with zero superfluid pinning and a crustal strain of no more than  $\sim 10^{-6}$ . The maximum amount of superfluid pinning allowed is of order  $10^{-10}$ .

### Remnant of SN 1987A

Middleditch et al. (2000a,b) have recently presented evidence for a 2.14ms optical pulsar in the remnant of SN 1987A. The source was observed intermittently between 1992 and 1997. A modulation in the phase and amplitude were detected, which the authors suggested may be due to free precession. The period of the modulation seemed to vary, spanning a range of 935s to 1430s. The amplitude of the phase modulation seemed to vary from  $\sim 48^\circ$  to  $\sim 60^\circ$ , although in some observing runs it was possibly zero. Middleditch et al. also suggest that the spin-down of the pulsar is due to the gravitational radiation reaction associated with the free precession.

We will examine the free precession and gravitational wave driven spin-down using our model. Crucially, the gravitational wave spin-down hypothesis can be tested: The ratio of the spin to modulation periods will enable us to calculate the deformation  $\Delta I_d$  of the star, while the phase modulation will allow us to calculate the wobble angle  $\theta$ . These can then be combined to give the gravitational wave spin-down, which can then be compared to the observed value of the frequency derivative.

First we will extract a value for the wobble angle using the amplitude of the phase residual,  $\Delta\Phi$ . This amplitude is highly variable, implying a variable wobble angle. At times the phase modulation seemed to disappear. If real, this disappearance would suggest that sometimes the star simply spins about its symmetry axis without precessing. When the modulation was present, values in the range  $\sim 48^\circ$  to  $\sim 60^\circ$  were found. Even if the spin-down were due entirely to a magnetic dipole, inequality (64) shows that the phase residual can be extracted while neglecting magnetic torque variations. Then, if  $\Delta\Phi$  was small, equation (66) would give the wobble angle (up to a factor of  $\tan \chi$ ). However,  $\Delta\Phi$  is not small, so the nonlinearised problem must be solved. This is not possible for a general value of  $\chi$ , but an example solution would be  $\chi = 59^\circ$ ,  $\theta = 80^\circ$  for  $\Delta\Phi = 60^\circ$  (equation 48). The key point is that  $\theta$  is not small, and the strains associated with such a large wobble angle would require a very high crustal breaking strain. Given that, to order of magnitude accuracy, the precession-induced strain is of order  $\theta\epsilon_{\text{fluid}}$ , we have a strain of order  $5 \times 10^{-2}$ . The breaking strain must be at least as large as this, exceeding even the

highest estimate of Ruderman (1992), weakening the free precession hypothesis.

Now use equation (69) to extract the reference oblateness. Using a modulation period of 1009s we find  $\epsilon_0 = 2.1 \times 10^{-3} M/R$ . Using equation (4) we find that the fluid oblateness is  $4.6 \times 10^{-2} R^3/M$ . The inequality (39) is violated (case I), even for high mass, small radius stars—the star is more nearly spherical than we would expect if its crust solidified at a rotation rate as high as 2.14ms. This discrepancy is resolved only if a significant portion of the star’s total moment of inertia participates in the free precession. Using equation (68) we see that we need  $I_0 = 0.33 I_{\text{star}}$  for  $\epsilon_0$  to be as large as  $\epsilon_{\text{fluid}}$ .

Now we will test the gravitational wave spin-down hypothesis. Balancing the rate of loss of angular momentum of the star against the gravitational flux we find (Cutler & Jones 2000):

$$\dot{\Omega} = \frac{32G}{5c^5} \Omega^5 \frac{(\Delta I_d)^2}{I_{\text{star}}} \sin^2 \theta (\cos^2 \theta + 16 \sin^2 \theta) \quad (76)$$

The quantity  $\Delta I_d$  can be extracted from observations:  $\Delta I_d/I_0 = P/P_{\text{fp}}$ , so that

$$\dot{\Omega} = \frac{32G}{5c^5} \Omega^5 \left( \frac{P}{P_{\text{fp}}} \right)^2 \frac{I_0^2}{I_{\text{star}}} \sin^2 \theta (\cos^2 \theta + 16 \sin^2 \theta) \quad (77)$$

Parameterising:

$$\left( \frac{\dot{f}}{20 \mu\text{Hz/day}} \right) = 1.5 \sin^2 \theta (\cos^2 \theta + 16 \sin^2 \theta) \left( \frac{2.14}{P} \right)^3 \left( \frac{10^3}{P_{\text{fp}}} \right)^2 \left( \frac{I_0/I_{\text{star}}}{0.33} \right)^2 M_{1.4} R_6^2. \quad (78)$$

For  $\theta \sim 1$  and  $I_0 = 0.33 I_{\text{star}}$  this is an order of magnitude *larger* than the observed value. However, if we were to disregard the  $\theta \sim 1$  derived from the phase modulation, we could use the above equation to calculate the wobble angle required for gravitational waves to provide angular momentum balance. We find  $\theta = 0.44$  radians =  $25^\circ$ . This corresponds to a crustal strain of order  $\theta \epsilon_{\text{fluid}} \sim 2 \times 10^{-2}$ . The breaking strain must be at least as large as this. This is an uncomfortably large value, exceeding even the highest estimates (Ruderman 1992). If the whole star participates in the free precession, so that  $I_0 = I_{\text{star}}$ , the wobble angle necessary to balance the spin-down is  $9^\circ$ , corresponding to a slightly more plausible breaking strain of  $8 \times 10^{-3}$ . Clearly, if the free precession and gravitational wave spin-down hypotheses are correct, our model points towards most or all of the star participating in the precession.

One of the main pieces of evidence Middleditch et al. cite to support the gravitational wave spin-down hypothesis is that the frequency derivative  $\dot{f}$  correlates rather well with the inverse square of the long modulation period  $P_{\text{fp}}$ . This is illustrated by figure 5 of Middleditch et al. (2000b), where  $\dot{f}$  varies by a factor of  $\sim 4$ , while  $P_{\text{fp}}$  varies by a factor of 2. As can be seen from equation (78), this correlation is indeed predicted by this model, *but only for a fixed wobble angle*. For the correlation to be perfect, the wobble angle would have to remain exactly constant. Referring to their figure, we see that with the exception of a single data point, all the error bars are consistent with the wobble angle remaining constant. The maximum fractional variation in the angular function  $\sin^2 \theta (\cos^2 \theta + 16 \sin^2 \theta)$  consistent with  $\dot{f}$  remaining

within the error bars is approximately 10%, corresponding to a variation away from  $\theta = 9^\circ$  of less than  $1^\circ$ , for instance. It is not easy to see how the (unknown) process that leads to a factor of two variation in the *size* of the deformation  $\Delta I_d$  could preserve the wobble angle to better than 10%.

To sum up, the large phase residual of around  $60^\circ$  cannot be accounted for: In such a fast spinning star it would correspond to a crustal breaking strain of around  $5 \times 10^{-2}$ , an implausibly large value. Setting this difficulty aside, in order to satisfy inequality (39) we found that at least one third of the star had to participate in the free precession. In order for this motion to provide the necessary gravitational spin-down torque an even larger portion of the star must precess. If the whole star precesses, the gravitational wave spin-down hypothesis requires a crustal breaking strain at least as large as  $8 \times 10^{-3}$ . If a smaller portion precesses, an even larger breaking strain is required.

### 7.3 Her X-1

Her X-1 is a 1.24s X-ray pulsar in a 1.7d binary orbit about a main-sequence star. A third periodicity of 35d has been measured. Some authors have attributed this to forced precession of the accretion disk (Petterson 1975; Gerend & Boynton 1976; Bisnovatyi-Kogan et al. 1990), others to free precession of the star (Brecher 1972; Shakura et al. 1998), while others argue for a combination of both (Trumper et al. 1986; Ketsaris et al. 2000). If the 35d periodicity is due to free precession the wobble angle must be large, of order unity (Shakura et al. 1998).

Equation (69) gives a reference oblateness of  $\epsilon_0 = 4.1 \times 10^{-4}$ , while equation (4) gives the star’s actual shape as  $\epsilon_{\text{fluid}} = 1.4 \times 10^{-7}$ . These values are consistent with inequality (39) (case II), so that the observations are consistent with a crust-only precession with zero superfluid pinning. The pinned superfluid component can make up no more than about  $10^{-8}$  of the total moment of inertia.

### 7.4 Summary and discussion of observations

We will now comment upon our findings, which are summarised in table 1. The key points are as follows:

- Only one observation (Crab, Lyne et al. 1988) did not fit our free precession model for any choice of parameters—the calculated reference shape was too nearly spherical to have been formed by solidification earlier in the Crab’s life when the star spun more rapidly than it does today.
- Only one observation (Crab, Čadež & Galičič 1996a) required superfluid pinning for its explanation. Assuming crust-only precession, this pinned component must make up a fraction  $10^{-5}$  of the total stellar moment of inertia.
- The remaining five observations could be made to fit our model with the pinned superfluid component set to zero, so that Coulomb forces provided the deformation in the moment of inertia tensor. Two observations required at least part of the interior fluid to participate in the free precession. Specifically, Vela required at least 6% of the total stellar moment of inertia to participate, while the SN 1987A remnant required at least 33%. The remaining observations were consistent with a crust-only free precession. The *maximum* amount of pinned superfluid consistent with the ob-

**Table 1.** This table summarises stellar parameters calculated from the spin and (proposed) free precession periods. The quantity  $\epsilon_{\text{eff}}$  is simply the ratio of these,  $P/P_{\text{fp}}$ . The actual oblateness  $\epsilon_{\text{fluid}}$  is calculated using equation (4). The quantity  $\epsilon_0$  is the reference oblateness as calculated when only the crust participates in the free precession, and there is no pinned superfluid (equation 69). The quantity  $I_{\text{SF}}/I_{\text{star}}$  is the fraction of the stellar moment of inertia made up of pinned superfluid, assuming that only the crust participates in the free precession, and that the reference oblateness is zero (equation 71). Key to references: (1) Lyne et al. (1988); (2) Čadež & Galičič (1996a); (3) Deshpande & McCulloch (1996); (4) Cordes (1993); (5) Stairs, Shemar & Lyne (2000); (6) Middleditch et al. (2000a); (7) Trümper et al. (1986).

Object	Reference	$\epsilon_{\text{eff}}$	$\epsilon_{\text{fluid}}$	$\epsilon_0$	$I_{\text{SF}}/I_{\text{star}}$
B0531+21 (Crab)	1	$6.4 \times 10^{-10}$	$2 \times 10^{-4}$	$6 \times 10^{-7}$	$9.6 \times 10^{-12}$
B0531+21 (Crab)	2	$5.5 \times 10^{-4}$	$1.9 \times 10^{-4}$	$5.5 \times 10^{-1}$	$8.3 \times 10^{-6}$
B0833-45 (Vela)	3	$6.2 \times 10^{-9}$	$2.7 \times 10^{-5}$	$6.2 \times 10^{-6}$	$9.3 \times 10^{-11}$
B1642-03	4	$4.5 \times 10^{-9}$	$1.3 \times 10^{-6}$	$4.5 \times 10^{-6}$	$6.8 \times 10^{-11}$
B1828-11	5	$4.7 \times 10^{-9}$	$1.3 \times 10^{-6}$	$4.7 \times 10^{-6}$	$7.1 \times 10^{-11}$
SN 1987A remnant	6	$2.1 \times 10^{-6}$	$4.6 \times 10^{-2}$	$2.1 \times 10^{-3}$	$3.2 \times 10^{-8}$
Her X-1	7	$4.1 \times 10^{-7}$	$1.4 \times 10^{-7}$	$4.1 \times 10^{-4}$	$6.2 \times 10^{-9}$

servations is typically  $\sim 10^{-10}$  of the stars’ total moment of inertia.

- We were able to explain two otherwise puzzling features of the Stairs et al. (2000) observation of PSR B1828-11 by assuming the dipole axis to lie nearly orthogonally to the deformation axis ( $\chi$  close to  $\pi/2$ ). Specifically, we were able to account for the presence of a strong 504d periodicity in the 1009d modulation, and the apparent discrepancy between the wobble angle as derived using the amplitude modulation and using the phase residuals.

As stated, two observations require more than just the crust to follow the free precession. However, we wish to go further, and ask the following: Are the observations consistent with part (or all) of the core liquid in *all* the neutron stars following the free precession? Taking the extreme case of total crust-core coupling, we set  $I_0$  equal to the total stellar moment of inertia in equations (68) and (70). This simply serves to increase the values of  $\epsilon_0$  and  $I_{\text{SF}}/I_{\text{star}}$  in the table by a factor of  $I_{\text{star}}/I_{\text{crust}}$ , i.e. by a factor of  $\approx 67M_{1.4}^2/R_6^4$  (equation 9).

In this case the qualitative conclusions that can be drawn are not very different from before. The Lyne et al. observation of the Crab is still inconsistent with the free precession model (although the reference oblateness is only a factor of 5 smaller than the fluid oblateness). The Čadež & Galičič observation of the Crab still requires a pinned superfluid, now making up a fraction  $10^{-3}$  of the total moment on inertia. As stated previously, the SN 1987A observation can *only* be explained assuming a large fluid component in the free precession. All the remaining observations continue to fit our model—the only change is that the maximum pinned superfluid component allowed is increased to values typically of order  $10^{-8}$ , still much smaller than the  $10^{-2}$  predicted by theory.

Another important question remains to be answered: Why are these stars precessing in the first place? What excited this motion? The two main candidates for isolated stars are glitches and electromagnetic torques. A glitch could excite free precession by occurring in a non-axisymmetric way, suddenly shifting the principal axis of the moment of inertia tensor while preserving the angular momentum (Link et al. 1998). Alternatively, the spin-down electromagnetic torque can amplify the wobble angle of an already precessing star

(Goldreich 1970). There may exist also an ‘anomalous’ electromagnetic torque (Jones 1988), which does not contribute to the spin-down, but will cause an initially non-precessing star to precess. Both glitches and electromagnetic torques are important for young stars, consistent with the rather young ages of the precession candidates. (All the isolated stars in table 1 have spin-down ages  $P/2\dot{P} \lesssim 10^5$  years, with the exception of B1642-03, which has a spin-down age of  $3 \times 10^6$  years). In the case of Her X-1, the accretion torque is the obvious source of wobble excitation (Lamb et al. 1975).

If electromagnetic torques are responsible, then we would expect almost all sufficiently young pulsars to display signs of free precession. In contrast, if glitching is responsible, we would expect to observe free precession in those stars which happened to have glitched recently, so that the precession has not yet been damped away. Only a fraction of the young pulsars show signs of free precession, favouring the glitch hypothesis.

## 8 CONCLUSIONS

As stated at the outset, our goal was to extract as much information as possible from the handful of pulsar candidates for free precession. To this end we built a free precession model capturing (we hope) the main features of the problem. Our model contained two coupling mechanisms between the crust and neutron fluid core. One was *inertial coupling*, where the fluid core effectively ‘pushed’ on the surrounding crust. The other was a frictional coupling due to the scattering of electrons off neutron vortices. We argued that even when these effects are taken into account, the neutron fluid core is not expected to follow the precession of the crust.

When we compared our model against the observations we found that the wobble angle of the candidates was typically small, less than a degree or so. Of greater interest was the information that might be extracted from the ratio of the spin and free precession periods,  $\epsilon_{\text{eff}}$ . This ratio depends on the details of the star’s structure, specifically on the geological history of the crust (parameterised by  $\epsilon_0$ ), on the amount of pinned superfluid ( $I_{\text{SF}}$ ), and on the portion of the star that participates in the free precession ( $I_0$ ). It was not possible to examine the three parameters independently, as they *all* contribute to the observed  $\epsilon_{\text{eff}}$  (see equation 31).

However, by assuming reasonable values for crustal strength ( $b$ ) and breaking strain ( $u_{\text{break}}$ ), a few general conclusions could be drawn. Firstly, if only the crust participates in the free precession, superfluid pinning need be invoked to explain only one of the observations. The others were consistent with no pinning at all, with an upper bound on  $I_{\text{SF}}$  typically of  $10^{-10}$  of the total stellar moment of inertia. In the (in our opinion less likely) case where the whole star precesses, the maximum pinned component was found to be typically  $10^{-8}$  of  $I_{\text{star}}$ . Both these values are many orders of magnitude smaller than predicted by some glitch theories. Clearly, if the observations considered here really do represent free precession, superfluid pinning theory, at least as it affects free precession, is in radical need of reworking.

### ACKNOWLEDGEMENTS

It is a pleasure to thank Curt Cutler and Bernard Schutz for stimulating discussions during the course of this work. This work was supported by PPARC grant PPA/G/1998/00606.

### REFERENCES

- Alpar A., Sauls J. A., 1988, *Ap. J.* **327** 723  
 Bisnovatyi-Kogan G. S., Kahabka P., 1993, *Astron. Astrophys.* **267** L43  
 Bisnovatyi-Kogan G. S., Mersov G. A., Sheffer E. K., 1990, *Sov. Astron.* **34(1)** 44  
 Bondi H., Gold T., 1955, *MNRAS* **115** 41  
 Brecher K., 1972, *Nature* **239** 325  
 Čadež A., Galičič M., 1996, *Astron. & Astrophys.* **306** 443  
 Čadež A., Galičič M., 1996, in Johnston S., Walker M. A., Bailes M., eds, ASP Conference Series, Vol 105, American Society of the Pacific  
 Čadež A., Galičič M., Calvini M., 1997, *Astron. & Astrophys.* **324** 1005  
 Cordes J. A., 1993, in Phillips J. A. and Thorsett J. E., eds ASP Conference Series, Vol 36  
 Cutler C., Jones D. I., 2000 To appear in *Phys. Rev. D*  
 Deshpande A. A., McCulloch P. M., 1996, in Johnston S., Walker M. A., Bailes M., eds, ASP Conference Series, Vol 105, American Society of the Pacific, p. 101  
 Deutsch A. J., 1955, *Annales d'Astrophysique* **18(1)** 1  
 Easson I., 1979, *Ap. J.* **228** 252  
 Gerend D. & Boynton P. E., 1976, *Ap. J.* **209** 562  
 Gil J. A., Jessner A., & Kramer M., 1993 *Astron. & Astrophys.* **271** L17  
 Glendenning N., 1995, *Ap. J.* **440** 881  
 Glendenning N., 1997, *Compact Stars*. Springer  
 Golden A. et al. 2000, To appear in *Astron. & Astrophys.*  
 Goldreich P., 1970, *Ap. J.* **160** L11  
 Jones D. I., 2000, PhD. Thesis, University of Wales, Cardiff  
 Jones P. B., 1988, *MNRAS* **235** 545  
 Ketsaris et al. 2000, astro-ph/0010035  
 Lamb D. Q., Lamb F. K., Pines D., Shaham J., 1975, *Ap. J.* **198** L21  
 Lamb H., 1952, *Hydrodynamics (Sixth Edition)*. Cambridge University Press  
 Landau L. D., Lifshitz E. M., 1976, *Mechanics*, 3rd Edition. Butterworth-Heinemann Ltd.  
 Link B., Franco L. M., Epstein R. I., 1998 *Ap. J.* **508** 838  
 Lyne A. G., Graham-Smith F., 1998, *Pulsar Astronomy*. Cambridge University Press  
 Lyne A. G., Pritchard R. S., Smith F. G., 1988, *MNRAS* **233** 667  
 Melatos A., 1999, *Ap. J.* **519** L77  
 Middleditch J., et al. 2000, *New Astronomy* **5** no. 5, 243  
 Middleditch J., et al. 2000, astro-ph/0010044  
 Munk W. H., McDonald G. J. F., 1960, *The Rotation of the Earth*. Cambridge University Press  
 Nelson R. W., Finn L. S., & Wasserman I., 1990, *Ap. J.* **348** 226  
 Petterson J. A., 1975, *Ap. J.* **210** L61  
 Pines D., Shaham J., 1972, *Phys. Earth and Planet. Interiors* **6** 103  
 Ravenhall D. G., Pethick C. J., 1994 *Ap. J.* **424** 846  
 Ruderman M., 1970, *Nature* **225** 838  
 Ruderman M., 1992, In *Structure and Evolution of Neutron Stars* p.353  
 Shaham J., 1977, *Ap. J.* **214** 251  
 Shakura N. I., Postnov K. A. & Prokhorov M. E., 1998, *Astron. & Astrophys.* **331** L37  
 Stairs I. H., Lyne A. G., Shemar S. L., 2000, *Nature* **406** 484  
 Trumper J., Kahabka P., Ogelman H., Pietsch W. & Voges W., 1986, *Ap. J.* **487** L63  
 Ushomirsky G., Cutler C., Bildsten L., 2000 astro-ph/0001136